Research Square

Preprints are preliminary reports that have not undergone peer review.
They should not be considered conclusive, used to inform clinical practice,
or referenced by the media as validated information.

Pyoverdine production and antagonistic activity of native wastewater Pseudomonas sp. strains against Colletotrichum sp. and Fusarium sp

Susana Ochoa-Agudelo

susana.ochoa@colmayor.edu.co

Institución Universitaria Colegio Mayor de Antioquia

León F. Toro-Navarro

Universidad de Antioquia

Howard Junca

Microbiomas Foundation

Andrés F. Villa-Restrepo

Universidad de Antioquia

J. Felipe Osorio-Tobón

Institución Universitaria Colegio Mayor de Antioquia

Research Article

Keywords: Pseudomonas spp., pyoverdine, siderophore, antifungal activity, metallophore, wastewater isolates

Posted Date: November 11th, 2026

DOI: https://doi.org/10.21203/rs.3.rs-11273157/v1

License: This work is licensed under a Creative Commons Attribution 4.0 International License.
Read Full License

Additional Declarations: No competing interests reported.

Pyoverdine production and antagonistic activity of native wastewater *Pseudomonas* sp. strains against *Colletotrichum* sp. and *Fusarium* sp.

Susana Ochoa-Agudelo[a], León F. Toro-Navarro[b], Howard Junca[c], Andrés F. Villa-Restrepo[b], J. Felipe Osorio-Tobón[a]

[a]*Facultad de Ciencias de la Salud, Institución Universitaria Colegio Mayor de Antioquia, Medellín, Colombia.*

[b]*Escuela de Microbiología, Grupo de Biotransformación, Universidad de Antioquia, Medellín, Colombia*

[c]*RG Microbial Ecology: Metabolism, Genomics & Evolution, Div. Ecogenomics & Holobionts, Microbiomas Foundation, Chía, Colombia*

*Corresponding Author:

E-mail*: susana.ochoa@colmayor.edu.co*

ORCID: https://orcid.org/0000-0001-5369-7137

Abstract

Pyoverdine, a primary siderophore secreted by *Pseudomonas* species, plays a crucial role in iron acquisition and phytopathogen biocontrol. This study evaluated pyoverdine production, iron-chelating capacity, and antifungal efficacy of native *Pseudomonas* sp. wastewater isolates P07 and P38 against *Colletotrichum* sp. and *Fusarium* sp. Media optimization showed that succinic acid is essential for pyoverdine synthesis, with medium M1 yielding high baseline levels (105.09 ± 1.63 µmol/L for P07). Formulating minimal media with reduced phosphate and moderate succinic acid (PM2) enhanced both pyoverdine production (up to 152.85 ± 4.43 µmol/L in P07 and 100.18 ± 7.04 µmol/L in P38) and iron-chelating capacity (up to 92.13 ± 0.85% PSU). In dual-challenge assays, strain P38 exhibited superior, iron-independent antagonism, suppressing *Colletotrichum* sp. (91.6%) and *Fusarium* sp. (91.39%). Microdilution bioassays revealed that P38 concentrated extracts inhibited *Colletotrichum* sp. (85.53%), demonstrating strong chemical antibiosis. Mass spectrometric analysis of the P38 extract revealed additional antifungal metabolites, including pyochelin, phenazines, and pyocyanin, confirming a multifaceted antagonistic profile. Native wastewater *Pseudomonas* sp. strains produce several bioactive compounds, including pyoverdines, which can markedly suppress the mycelial growth of key phytopathogenic fungi. These findings confirm that strain P38's antagonism extends beyond pyoverdine-mediated iron starvation to a rich, co-regulated secretome, establishing strain P38 as a promising candidate for bio-fungicidal tools in sustainable agriculture.

Keywords: *Pseudomonas spp.; pyoverdine; siderophore; antifungal activity; metallophore; wastewater isolates.*

Statements and Declarations

Financial disclosure

Susana Ochoa-Agudelo and J. Felipe Osorio-Tobón thank the Institución Universitaria Colegio Mayor de Antioquia for funding this work through the 2021 internal call for proposals.

Ethical approval

Not applicable.

Conflict of interest

The authors confirm no conflicts of interest regarding this paper.

Author contributions

Susana Ochoa-Agudelo performed research & funding resources, investigation, formal analysis, and writing the original draft. León F. Toro-Navarro, Howard Junca, and Andrés F. Villa-Restrepo contributed to conceptualization, review & editing. J. Felipe Osorio-Tobón contributed to conceptualization, formal analysis, and writing, review & editing.

1. Introduction

Microorganisms, including bacteria, cyanobacteria, archaea, fungi, yeasts, algae, and certain protozoa, can synthesize diverse bioactive compounds such as terpenoids, steroids, polyketides, fatty acid derivatives, alkaloids, non-ribosomal peptides, and shikimate-derived compounds (Abdel-Razek et al., 2020). These compounds are widely recognized for their antimicrobial, antioxidant, anticancer, antitumor, and anti-inflammatory properties (Abdelghani et al., 2021; Abdel-Razek et al., 2020; Rani et al., 2021).

Among bacteria, the genus *Pseudomonas* is widely distributed throughout soil, aquatic environments, and diverse ecological niches. *Pseudomonas* spp. are renowned for their high competitive and adaptive capacity across varied habitats (Ghssein & Ezzeddine, 2022; Jeong et al., 2023). Moreover, owing to its physiological and metabolic versatility, the genius holds significant potential for applications in bioremediation and sustainable agriculture (Swayambhu et al., 2021). In agricultural settings, *Pseudomonas* promotes plant growth and serves as an effective biocontrol agent against various phytopathogens, including bacteria and filamentous fungi such as *Ralstonia* sp., *Fusarium* sp., and *Aspergillus* sp. (Abdelghani et al., 2021; de Alvindia & Mangoba, 2020; Islam et al., 2018; Kipgen et al., 2021; Rani et al., 2021).

Pathogenic fungi such as *Colletotrichum* sp. and *Fusarium* sp. cause several yield losses in global agriculture. *Colletotrichum* sp. is capable of infecting numerous host plants, causing destructive anthracnose in crops such as bananas, mangoes, avocados, strawberries, and garlic (Chung et al., 2020; de Alvindia & Mangoba, 2020; Dutta et al., 2022; Kim et al., 2023; Ma et al., 2025). Similarly, *Fusarium* sp. enters through the plant's roots, invades the vascular tissue, and blocks the transport of water and nutrients, causing necrosis and affecting crops such as tomatoes, spinach, and beans (Gyawali et al., 2025; Purohit et al., 2021).

Pyoverdines (PVDs) are low-molecular-weight siderophores produced by bacteria, including *Pseudomonas*. Composed of a chromophore, an acyl side chain, and a variable peptide chain, these molecules have attracted attention for their potential applications in bioremediation and biological control (Dell'Anno et al., 2022) . For example, siderophores produced by *Pseudomonas putida* have shown potent *in vitro* antagonistic effects against the phytopathogenic fungus *Aspergillus niger* (Hussein & Joo, 2017). Thus, promoting PVD synthesis represents a valuable approach for developing sustainable alternatives to inhibit the growth of key fungal pathogens.

The composition of the culture medium is a critical factor in influencing PVD synthesis and chelating capacity. While minimal media (such as MMS) support baseline PVD production, modifications in carbon and nitrogen sources, as well as amino acid supplementation, can significantly enhance PVD yield (Vindeirinho et al., 2021). In culture media optimization, organic acids (such as citric and succinic acid) and casamino acids (CAA) are frequently evaluated as carbon and nitrogen sources because they participate directly in PVD biosynthesis (Sarvepalli et al., 2023; Soares, 2022). In this context, the present study evaluated different carbon and nitrogen sources for PVD production and chelating capacity by native *Pseudomonas* sp. strains isolated from wastewater, as well as their antagonistic potential against *Colletotrichum* sp. and *Fusarium* sp.

2. Materials and Methods

2.1. Microorganisms

Two *Pseudomonas* strains (P07 and P38), isolated from wastewater and deposited in the Institución Universitaria Colegio Mayor de Antioquia University culture collection (CEMBIO), were revived in LB medium at 32 ± 2 °C for 24 hours. Strains were characterized using the 16S rDNA gene in previous work (Bedoya Vélez et al., 2019). The microbial growth was verified by observing colony morphotypes, pigment production, and fluorescence. Gram staining confirmed Gram-negative bacilli using optical microscopy. Viable strains were cryopreserved in aliquots with BHI broth (Merck®) until experimental use.

CEMBIO supplied the wild phytopathogenic fungi *Colletotrichum* sp. and *Fusarium* sp., which were inoculated onto PDA agar and incubated at 25 ± 2 °C for 5 days. Radial growth of the mycelium was observed, and its identity was confirmed by examining its macroscopic and microscopic morphology (Islam et al., 2018; Song et al., 2021).

2.2. Inoculum preparation

Fresh cultures of each strain were used as inoculum to prepare cell suspensions adjusted to a McFarland 0.5 standard (1.5×10^8 cells/mL). A concentration of 5 % (v/v) relative to the final volume was used (Vindeirinho et al., 2021). A portion of fresh mycelium of *Colletotrichum* sp. and *Fusarium* sp. were taken from each isolate and incubated at 25 ± 2 °C for 5 days on PDA agar. Subsequently, depending on the experimental requirements, a conidia suspension was prepared, and the conidia were counted using a Neubauer chamber until

a concentration of 1.5×10^5 conidia/mL was reached (Sasirekha & Srividya, 2016). The suspension was stored at room temperature until use.

2.3. Effect of carbon and nitrogen source on PVD production and chelating capacity

Initially, the strains were incubated for 24 h in MMS medium using various carbon and nitrogen sources. Succinic acid and citric acid were used as carbon sources, whereas ammonium sulfate and Casamino acids (CAA) were used as nitrogen sources. MMS medium was prepared as follows: 6 g/L potassium phosphate, 3 g/L dihydrogen phosphate, and 0.2 g/L magnesium sulfate. Different concentrations of ammonium sulfate, CAA, succinic acid, and citric acid were evaluated as shown in Table 1.

Table 1. Chemical composition (g/L) of culture media (M1-M4) evaluated for pyoverdine production and chelating capacity using different carbon and nitrogen sources.

Component	Culture media			
	M1	M2	M3	M4
	Concentration (g/L)			
Ammonium sulfate	1.0	1.0	-	-
Casamino acids (CAA)	-	-	1.0	1.0
Succinic acid	4.0	-	4.0	-
Citric acid	-	4.0	-	4.0

2.4. Quantification of PVD and iron-chelating capacity

An aliquot was taken from each sample and centrifuged at 10,000 rpm for 10 minutes. The supernatant was used to estimate siderophore production and chelating capacity. Siderophore production was measured by absorbance at a wavelength of 405 nm in a spectrophotometer (Thermo Scientific™, Genesys 180 UV-Vis, Madison, USA), according to Beer's Law (Vindeirinho et al., 2021). Siderophore activity was quantitatively estimated using the CAS (Chromo Azurol S) reagent technique at 630 nm (Schwyn & Neilands, 1987). The reference sample was prepared as described above, but using 1 mL of uninoculated medium (Murakami et al., 2021). All assays were performed in triplicate, using inoculum-free medium as a negative control. The iron-chelating capacity (or siderophore activity) was calculated as the percentage of siderophore units (PSU), using equation (E1):

$$\text{PSU} = \frac{Ar - As}{Ar} * 100 \quad \text{(E1)}$$

Where *Ar* represents the absorbance of the reference, and *As* represents the absorbance of the sample.

2.5. Preparation of crude PVD-rich extract

The crude PVD-rich extract was obtained using the methodology reported by Bello et al. (2006), with minor modifications. Briefly, three volumes of free-cell culture supernatant were mixed with one volume of methanol, then four volumes of 96% ethanol were added under thorough agitation. The mixture was incubated at 4 °C for 3 to 5 days until precipitation occurred. After separating the precipitate, the supernatant was transferred to an amber container and concentrated by rotary evaporation at 60 °C. The dried extract was freeze-dried at -22 °C and 0.75 mbar for 24 hours and stored at -20 °C until further use.

2.6. Antagonistic activity by dual-challenge test

Fresh bacterial cultures of each *Pseudomonas* sp. strain were grown in LB medium at 32 ± 2 °C for 24 h. Antagonistic assays were performed on potato dextrose agar (PDA) plates, with and without iron supplementation, to determine whether iron availability regulates PVD synthesis and affects fungal suppression (Sasirekha & Srividya, 2016). Initially, PDA plates were inoculated at the center with a 5-mm agar plug of *Colletotrichum* sp. or *Fusarium* sp. After 24 hours of fungal incubation, each *Pseudomonas* sp. strain was streaked onto the agar surface at points equidistant from the central fungal inoculum (Islam et al., 2018). After 3 days of incubation at 28 ± 2 °C, the percentage of dual-challenge growth inhibition (%INH_{dual}) was determined using Equation 2:

$$\%INH_{dual} = \frac{(rc - rt)}{rc} \times 100 \quad (2)$$

Where *rc* is the radial mycelial growth of the fungus in the control plate (without bacterial antagonist), and *rt* is the radial mycelial growth of the fungus in the presence of *Pseudomonas* sp. strain.

2.7. Antagonistic activity by broth microdilution assay

Fungal growth inhibition by culture supernatants and PVD-rich extracts was evaluated in 96-well microplates following the Clinical Laboratory Standards (NCCLS) (Tapia P., 2009), with minor modifications.

Briefly, each well received 80 µL of Sabouraud dextrose broth, 10 µL of cell-free supernatant or concentrated extract, and 10 µL of conidial suspension (1.5 x 10^5 conidia/mL). Wells containing conidia in culture medium without extract served as positive growth controls, while uninoculated medium wells served as negative controls. All assays were conducted in triplicate. Plates were incubated at 28 ± 2 °C for 5 days. Fungal absorbance was measured at 530 nm using a microplate spectrophotometer, and the percentage of growth inhibition (%INH) was calculated using Equation 3:

$$\%INH = \frac{(A_0 - A_T)}{A_0} \times 100 \quad (3)$$

Where Ao is the absorbance of the untreated growth control, and A_T is the absorbance of the treated well.

2.8. Metabolite characterization by UHPLC-HR-MS/MS

Chemical profiling of the PVD-rich crude extract was performed using an UltiMate 3000 UHPLC system (Thermo Fisher, Waltham, MA, USA) equipped with a binary RS pump, an XRS open-loop autosampler, and a temperature-controlled column oven. Chromatographic separation was achieved at 25 °C using a Hypersil GOLD™ aQ C18 Polar Endcapped column (100 Å, 1.8 µm, 2.1 × 100 mm, Waters, Milford, USA). The mobile phases consisted of A) water containing 0.1% (v/v) formic acid and B) acetonitrile containing 0.1% (v/v) formic acid. Chromatographic separation was conducted at a constant flow rate of 0.4 mL/min using the following gradient: isocratic 4 % B from 0.525 to 5 min; linear increase to 11 % B at 5.25 min; linear increase to 95 % B at 7.0 min; held at 95 % B until 7 min; return to the initial conditions of 4 % B between 7 and 10 min; and, finally, an equilibration period for 4.5 min (Rehm et al., 2022).

UHPLC was coupled to an electrospray ionization mass spectrometer in positive ion mode (H-ESI, Thermo Fisher Scientific, Waltham, MA, USA), operated in full-scan mode with a resolution of 120 000 (FWHM, m/z 200) and an acquisition range of 140–2000 m/z. Instrumental parameters included a normalized collision energy (NCE) of 50%, HCD mode, an AIF range of 133.9–1,900 m/z, and positive polarity at 3,500 V. The samples were analyzed under two different conditions: 1) full-scan (FS) / All-ion fragmentation (AIF), high-energy collision-induced dissociation of all ionized molecules without prior mass filtering, 140 000 full width at half maximum (FWHM) resolution at m/z 200, Itmax 500 ms, AGC target 3e6 for FS and AIF, mass ranges of m/z 140–2000 (FS) and m/z 133,3–1900 (AIF), and normalized collision energy (NCE) of 50; 2) FS/alternative parallel reaction monitoring (PRM), 70 000 FWHM resolution with ITmax 200 ms (FS).

External calibration was performed prior to analysis using Pierce LTQ ESI positive-ion standard solution (Thermo Fisher Scientific, Waltham, MA, USA) to maintain accuracy below 5 ppm. Data acquisition and spectral processing were conducted using Compound Discoverer 3.3 (online), and complementary analysis was conducted using the *Pseudomonas aeruginosa* Metabolome Database (PAMBD; version 1.0). Excel was used to analyze and predict precursor and fragment m/z values for PVD-type siderophores and related molecules.

2.9. Statistical analysis

All experimental assays (PVD concentration, iron-chelating capacity, and fungal growth inhibition) were performed in independent triplicates (n=3), and the data are presented as the mean ± standard deviation (SD). After confirming compliance with the assumptions of normality, homoscedasticity, and independence, data were subjected to one-way analysis of variance (ANOVA) followed by Tukey's multiple range test ($p < 0.05$) to evaluate differences among media formulations and antagonistic activity treatments. All statistical analyses were conducted using Minitab® software (version 16).

3. Results and discussion

3.1. Substrate effect on PVD production

Evaluation of PVD production from *Pseudomonas* spp. strains P07 and P38 cultured in media with modified carbon and nitrogen sources revealed statistically significant differences ($p < 0.05$; Figure 1A). Strain P07 produced the highest PVD concentration in conventional medium M1 (succinic acid + ammonium sulfate; 105.09 ± 1.63 µmol/L), whereas medium M4 showed significantly lower levels (16.08 ± 1.16 µmol/L). Conversely, strain P38 exhibited its highest PVD concentration in media M2 and M3, with no statistically significant differences between them (36.90 ± 2.03 and 37.55 ± 0.19 µmol/L, respectively), followed by media M1 and M4 (33.41 ± 0.16 and 30.34 ± 0.97 µmol/L, respectively). For both isolates, PVD yield in medium M4 was significantly lower than in M1, indicating that succinic acid is essential for optimal PVD biosynthesis, particularly in strain P07, which demonstrated a strong metabolic affinity for succinate-driven secondary metabolite production. In contrast, variations in carbon and nitrogen sources induced less pronounced fluctuations in PVD synthesis in strain P38.

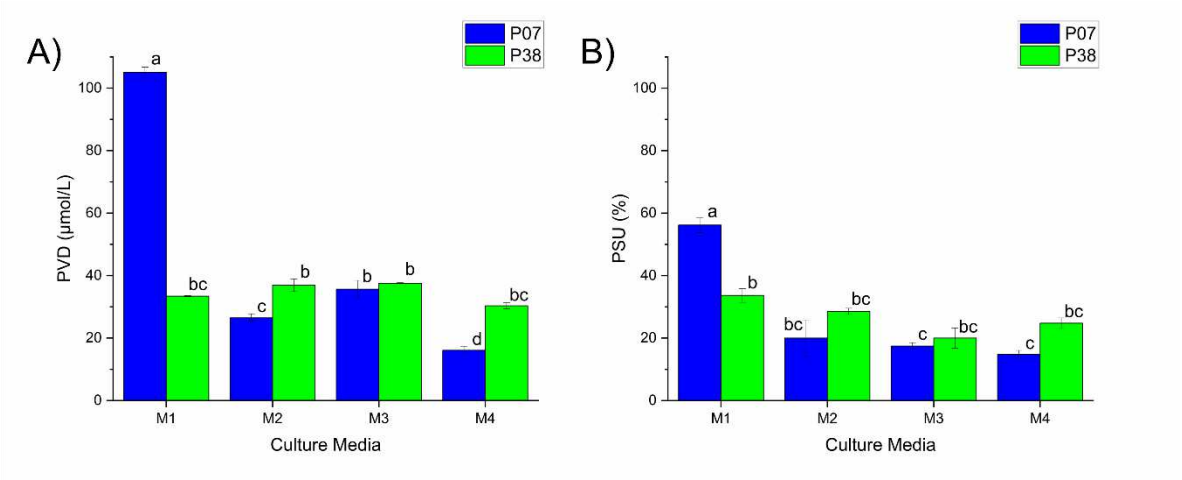


Figure 1. PVD production and iron-chelating capacity (PSU) by native Pseudomonas sp. strains P07 and P38 cultured in minimal media (M1-M4), varying carbon and nitrogen sources. Data represent the mean ± SD (n = 3). Different lowercase letters above the bars indicate statistically significant differences according to Tukey´s test ($p < 0.05$).

Furthermore, modifying the nitrogen source had a more pronounced impact on iron-chelating capacity (measured as PSU) in strain P07 than in strain P38 (Figure 1B). Conventional medium formulation M1 (succinic acid + ammonium sulfate) yielded significantly higher chelating capacity than all other formulations for both isolates ($p < 0.05$), though overall activity was substantially higher in strain P07 (56.18 ± 2.42%) than in strain P38 (28.56 ± 0.99%). For both strains, replacing ammonium with casamino acids (CAA; media M3 and M4) markedly suppressed chelating capacity regardless of the carbon source (Figure 1B).

Regarding the carbon source, gluconeogenic substrates such as succinic acid are widely documented to promote PVD biosynthesis (Soares, 2022). Vindeirinho et al. (2021) demonstrated that moderate succinic acid concentrations stimulate PVD synthesis, whereas excessive levels favor biomass accumulation over siderophore secretion. In contrast, the literature reports contradictory effects for citric acid, depending on co-substrate availability. For example, Sarvepalli et al. (2023) observed that citric acid stimulates PVD production only when paired with an alternative carbon source.

While some studies note positive effects of citric acid (Kumar & Tiwari, 2017) and others report negligible impacts (Nair et al., 2007) our findings reflect this lack of consensus. Media formulated with citric acid as the sole carbon source (M2 and M4) did not enhance PVD yield, suggesting that these strains

preferentially channeled citric acid toward cell growth rather than siderophore biosynthesis. This heterogeneous, strain-dependent response underscores the highly specific metabolic regulation of secondary metabolism in individual *Pseudomonas* isolates.

Although inorganic ammonium sources generally stimulate PVD synthesis compared to organic or nitrate nitrogen sources (Soares, 2022), modifying the nitrogen supply in this study yielded variable outcomes. Substituting ammonium with CAA (M1 vs M3) did not increase PVD yield, confirming that the conventional M1 formulation remains the most effective medium for optimizing pyoverdine synthesis in subsequent assays.

Consequently, the conventional MMS formulation containing succinic acid and an ammonium source was retained as the baseline medium for optimizing PVD synthesis. To evaluate the combined effects of phosphate concentration and succinic acid availability on PVD production and iron-chelating capacity, three modified formulations (PM1-PM3) were evaluated (Table 2). Bacterial strains were cultured for 24 h in MMS medium containing fixed concentrations of magnesium sulfate (0.2 g/L) and ammonium sulfate (1 g/L), while the concentrations of dipotassium hydrogen phosphate, potassium dihydrogen phosphate, and succinic acid were varied as shown in Table 2.

Table 2. Chemical composition (g /L) of culture media (PM1-PM3) evaluated for pyoverdine production and chelating capacity using different phosphate and succinic acid concentrations.

Component	Culture media		
	PM1	PM2	PM3
	Concentration (g/L)		
Potassium phosphate	6.0	2.0	2.0
Dihydrogen phosphate	3.0	0.4	0.4
Succinic acid	4.0	4.0	6.0

3.2. Effect of succinic acid and phosphate concentrations on PVD production and iron-chelating capacity

Modifying the composition significantly affected both PVD production and iron-chelating capacity ($p < 0.05$; Figures 2A and 2B). Medium PM1 supported high PVD yield in strain P07, whereas mediums PM2 and PM3 promoted maximum chelating capacity across both isolates. For strain P07, PVD concentrations ranged from 80.68 ± 12.91 to 152.85 ± 4.43 µmol/L, with the highest levels observed in media PM1 and PM2 as shown in Figure 2A, where succinic acid concentration was maintained at 4 g/L. However, increasing succinic acid to

6 g/L under reduced-phosphate conditions (medium PM3) led to a marked decline in PVD yield in medium PM1 (80.68 ± 12.91 µmol/L). In contrast, strain P38 exhibited its lowest PVD yield in medium PM1 (22.95 ± 1.59 µmol/L) but achieved its peak PVD production in medium PM2 (100,18 ± 7,04 µmol/L), demonstrating that phosphating reduction strongly stimulated PVD synthesis in this isolate (Figure 2A).

The percentage of siderophore units also varied significantly among formulations ($p < 0.05$; Figure 2B). Strain P07 attained chelating capacity values between 65.1 ± 7.54 and 92.13 ± 0.85% PSU. Decreasing the phosphate concentration enhanced chelating capacity, with medium PM2 yielding the highest activity (92.13 ± 0.85% PSU). For strain P38, PSU values ranged from 31.9 ± 7.01 to 79.37 ± 0.23% PSU; reducing the phosphate content in formulation PM2 resulted in more than a two-fold increase in chelating capacity (79.37 ± 0.23% PSU; Figure 2b).

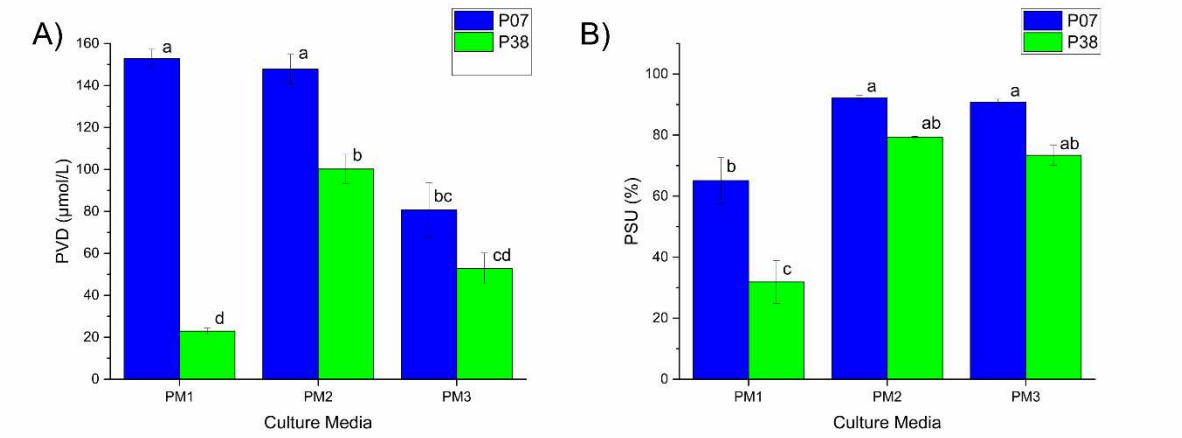


Figure 2. PVD production and iron-chelating capacity (PSU) by native Pseudomonas sp. strains P07 and P38 cultured in minimal media (PM1-PM3), varying phosphate concentrations and succinic acid availability. Data represent the mean ± SD (n = 3). Different lowercase letters above the bars indicate statistically significant differences according to Tukey´s test ($p < 0.05$).

Overall, while baseline PVD secretion differed between strains, the highest chelating capacity was consistently observed in medium PM2 (low phosphate, 4.0 g/L succinic acid), indicating enhanced PVD synthesis and functional stability. This trend aligns with observations reported by Vindeirinho et al. (2021) for *Pseudomonas fluorescens*, where reduced phosphate levels stabilized PVD molecules and enhanced iron-chelating efficiency. Furthermore, Soares (2022) noted that combining succinic acid as a gluconeogenic carbon source with phosphate limitation creates optimal physiological conditions for secondary metabolite production and

bioactivity. Consequently, these findings confirm that maintaining low phosphate availability, paired with a moderate succinic acid concentration (medium PM2), effectively optimizes both pyoverdine yield and iron-chelating capacity in native *Pseudomonas* sp. isolates.

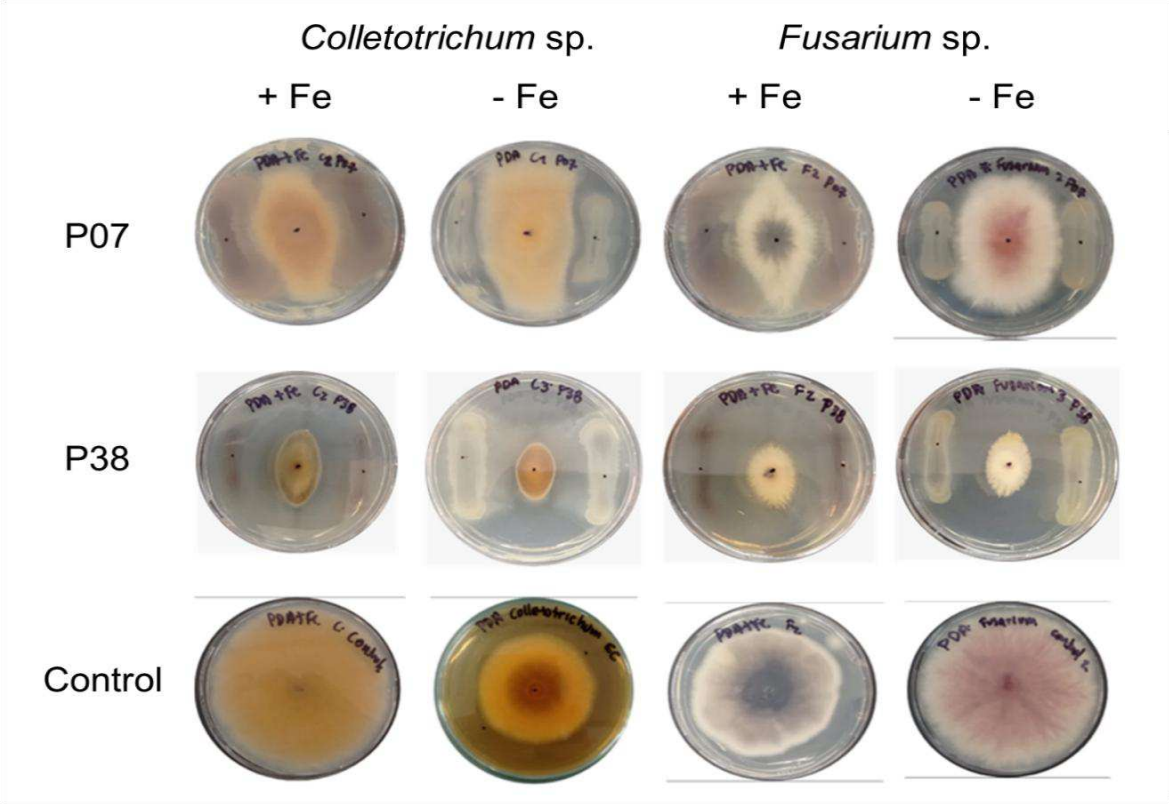


Figure 3. Mycelial growth inhibition of *Colletotrichum* sp. and *Fusarium* sp. by *Pseudomonas* sp. strains P07 and P38.

3.3. Antagonistic activity by dual challenge test

Qualitative results from the dual challenge assay demonstrated clear inhibition of fungal growth by *Pseudomonas* strains P07 and P38 against *Colletotrichum* sp. and *Fusarium* sp. under both iron-sufficient (+Fe) and iron-limited (-Fe) conditions (Figure 3). Radial mycelial growth of both phytopathogens was strongly restricted in the presence of strain P38 regardless of iron supplementation, with a distinctive white halo surrounding the bacterial colonies indicative of biofilm formation. In contrast, strain P07 exhibited pathogen-dependent activity, displaying significantly greater inhibition against *Colletotrichum* sp. in iron-supplemented media.

The antagonistic activity of *Pseudomonas* strains P07 and P38 against *Colletotrichum* sp. and *Fusarium* sp. was significantly influenced by both the specific bacterial strain and iron availability in the culture media. Overall, strain P38 exhibited a superior and robust biocontrol profile compared to strain P07, consistently achieving high mycelial growth inhibition levels ranging from 88% to 92% across all tested scenarios.

Specifically, in dual-challenge assays, the strain P38 suppressed the growth of *Colletotrichum* sp. and *Fusarium* sp. by 91%. Notably, the strain P38 maintained high inhibitory rates (88.08% to 91.26%) regardless of the presence (+Fe) or absence (-Fe) of iron in the medium (Figure 4), indicating an antagonistic effect independent of iron starvation. In contrast, strain P07 displayed moderate inhibition rates ranging from 44.71% to 64.04%, with specific dual-test inhibition values of 44.9% against *Colletotrichum* sp. and 55.1% against *Fusarium* sp. For strain P07, the highest antagonistic activity against *Fusarium* sp. showed no significant differences between iron-replete and iron-limited treatments (Figure 4).

The inhibitory performance of strain P38 surpasses several previously reported values for biocontrol *Pseudomonas* isolates. For instance, Kejela et al. (2017) observed a 50.30% inhibition of *Fusarium oxysporum* by *Pseudomonas* sp. Similarly, Ch'ng et al. (2022) reported inhibition rates exceeding 40.0% against *Fusarium oxysporum* f. sp. *cubense* using siderophore-producing *Pseudomonas* strains. On the other hand, Islam et al. (2018) achieved up to 90.20% reduction in *Fusarium* mycelial biomass using a *Pseudomonas aeruginosa* cultured in King´s B medium, which aligns closely with the high bioactivity demonstrated by P38 in this study. Furthermore, Kim et al. (2023) demonstrated that secondary metabolites such as cyclic peptides produced by *Pseudomonas sesami* effectively impair mycelial development in *Colletotrichum* species.

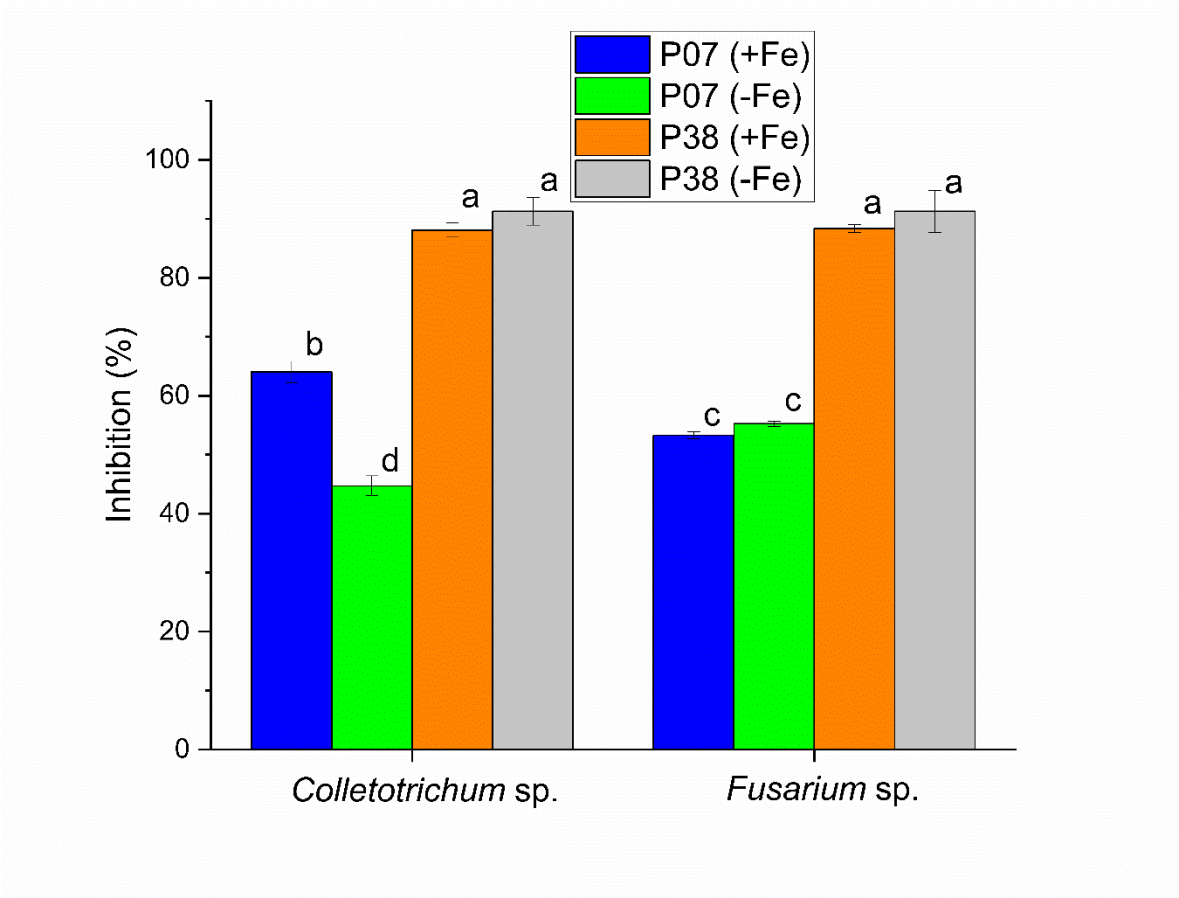


Figure 4. Percentage of mycelial growth inhibition (%) of *Colletotrichum* sp. and *Fusarium* sp. by *Pseudomonas* sp. strains P07 and P38 in dual-challenge assays under iron-sufficient (+Fe) and iron-limited (–Fe) conditions24. Data represent the mean ± SD (n = 3). Bars sharing different lowercase letters differ significantly according to Tukey's test ($p < 0.05$).

These results indicate that the fungal efficacy of strains P07 and P38 does not rely exclusively on pyoverdine-mediated iron competition. Antagonism in dual-culture assays generally manifests through a combination of physiological effects—such as direct competition for space and nutrients—and chemical effects mediated by diffusible bioactive metabolites. Fluorescent pseudomonads deploy a multifaceted biocontrol arsenal, including biofilms, phenazines, pyocyanin, and lipopeptides, during microbial interactions (Baukova et al., 2024; Díaz-Pérez et al., 2022). Consequently, while siderophore synthesis contributes to iron chelation, the strong, iron—independent inhibition exhibited by strain P38 confirms the production of additional, highly active extracellular antifungal compounds.

3.4. Antagonistic activity in a microdilution assay

The antagonistic efficacy of native *Pseudomonas* sp. strains P07 and P38 was further evaluated using broth microdilution assays to determine the inhibitory potential of cell-free supernatants and concentrated PVD extracts derived from conventional (PM1) and phosphate—modified (PM2) minimal media. This approach allowed decoupling of physiological competition (direct cell—to—cell contact) from purely chemical inhibition mediated by secreted extracellular metabolites.

PVD quantification and iron—chelating capacity (%PSU) varied significantly depending on the culture formulation, the strain, and the physical state of the metabolite preparation (Figure 5). Concentrated extracts consistently yielded the highest PVD concentrations regardless of the strain, with formulation PM2 acting as a superior inducer (Figure 5A). Specifically, concentrated PM2 extracts reached peak PVD levels of 207.58 ± 9.31 µmol/L for strain P07 and 219.76 ± 7.89 µmol/L for strain P38. In contrast, strain P38 produced lower baseline PVD levels in PM1 supernatant (22.95 ± 1.59 µmol/L), which increased to 135.72 ± 11.36 µmol/L in the concentrated extract. For strain P07, concentrated extracts from both PM1 and PM2 maintained consistently high PVD values (203.68 ± 7.40 and 207.58 ± 9.31 µmol/L, respectively).

Regarding chelating capacity, PM2 supernatants achieved the highest iron—chelating activity, exhibiting 93.3% PSU for P07 and 85.97% PSU for P38 (Figure 5B). Although concentration increased PVD detection spectrophotometrically, it did not always result in a proportional increase in iron—chelating unit values, particularly for strain P38 in PM2. This discrepancy indicates that measured PVD concentration does not linearly correlate with functional iron—binding affinity, a phenomenon that aligns with findings by Murakami et al. (2021) who noted that culture media components and non—specific spectrophotometric absorption can decouple PVD yield from actual iron—chelating efficiency.

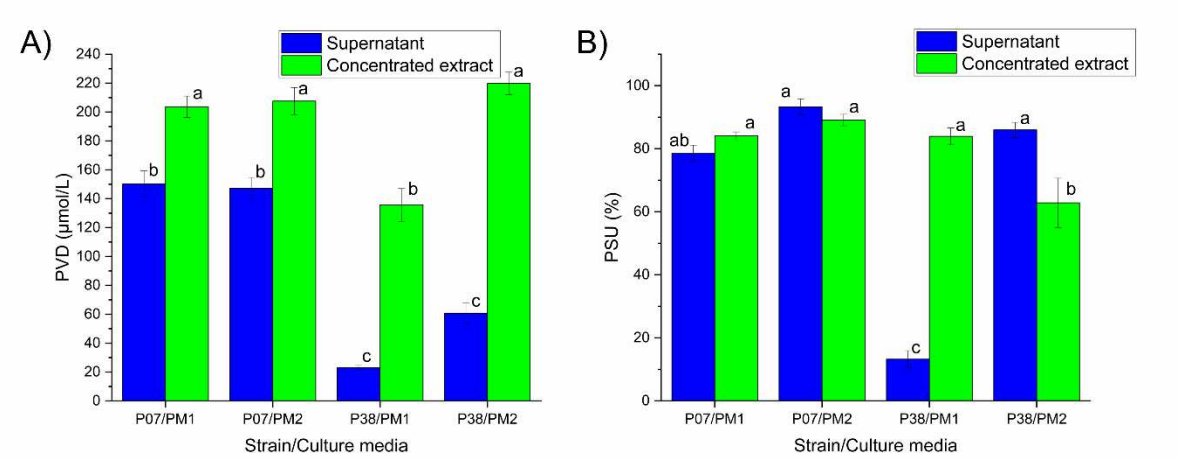


Figure 5. PVD concentration and percentage of mycelial growth inhibition (%) of supernatant and concentrated extract of native *Pseudomonas* sp. strains P07 and P38 under different culture medium formulations (PM1 and PM2). Data represent the mean ± SD (n = 3). Bars sharing different lowercase letters differ significantly according to Tukey's test ($p < 0.05$).

Microdilution bioassays against *Colletotrichum* sp. and *Fusarium* sp. revealed distinct pathogen—specific susceptibility profiles when comparing live dual challenge tests, cell—free supernatants, and concentrated extracts (Table 3). Against *Colletotrichum* sp., concentrating the extracellular metabolites of strain P38 significantly enhanced growth inhibition from53.62 ± 5.92% (supernatant) to 85.53 ± 5.15% (concentrated extract), closely mirroring the high efficacy observed in direct dual—culture competition (91.61 ± 3.55%). For strain P07, both the cell—free supernatant (62.45 ± 5.92%) and the concentrated extract (61.81 ± 4.55%) surpassed inhibition in live dual assays (44.90 ± 1.54%), confirming that *Colletotrichum* sp. is particularly sensitive to diffusible bioactive compounds present in the bacterial secretions.

Conversely, antifungal activity against *Fusarium* sp. was predominantly driven by direct microbial competition (Table 3). Dual challenge assays with living cells yielded the strongest suppression of *Fusarium* sp. for both strains (91.39 ± 4.66% for P38 and 55.10 ± 2.23% for P07). Exposure to cell—free supernatants or concentrated extracts resulted in lower inhibition rates (16.96% to 31.87), indicating that diffusible chemical compounds alone exert a diminished effect against *Fusarium* sp. when diluted or separated from active cell growth.

Table 3. Antagonistic activity of native *Pseudomonas* strains (cell—free supernatant and concentrated extract from strains) against *Colletotrichum* sp. and *Fusarium* sp.

Strain		*Colletotrichum* sp.	*Fusarium* sp.
P07	Dual test	44.9 ± 1.54[b]	55.1 ± 2.23[a]
	Supernatant	62.45 ± 5.92[a]	31.87 ± 5.95[b]
	Concentrated Extract	61.81 ± 4.55[a]	16.96 ± 3.27[c]
P38	Dual test	91.61 ± 3.55[a]	91.39 ± 4.66[a]
	Supernatant	53.62 ± 5.92[c]	26.61 ± 2.72[b]
	Concentrated Extract	85.53 ± 5.15[ab]	22.83 ± 3.71[b]

These findings demonstrate that pseudomonad antagonism operates through a dual mechanism involving competition for physiological space and nutrients and chemical antibiosis. While concentrated metabolites (such as PVD and associated bioactive molecules) strongly suppressed *Colletotrichum* sp. growth, *Fusarium* sp. biocontrol requires direct, active microbial interaction. Consequently, strain P38, whose concentrated extract retained potent antifungal activity against *Colletotrichum* sp. (85.53%), represents the most promising candidate for extract—based biocontrol formulations.

3.5. Characterization of the extract by HPLC—MS

Non—targeted metabolomic profiling via HPLC— MS was conducted on the concentrated extracellular extract of strain P38 to identify the specific bioactive metabolites responsible for its potent, multi—target fungal activity. Chromatographic and mass spectrophometric analysis identified 37 distinct chemical features in the active fraction. Comparing these mass—to—charge (m/z) signatures against the *Pseudomonas aeruginosa* metabolome database (PAMDB, version 1.0) yielded putative structural assignments for 90 secondary metabolites and metabolic intermediates (Table 4).

The chemical profile of strain P38 revealed a rich array of secondary metabolites regulated by quorum—sensing systems, particularly alkylquinolones belonging to the *Pseudomonas* quinolone signal (PQS) network, such as C11—PQS (316.1 m/z). In fluorescent pseudomonads, C11—PQS acts as a master regulator that modulates the biosynthesis of PVD, pyocyanin (PYO), and 1—1—phenacincarboxylic acid (PCA), while simultaneously functioning as a weak iron chelator that fine—tunes siderophore expression and virulence phenotypes.

Among the identified antifungal compounds, phenazines and phenazine—derived pigments featured prominently. Pyocyanin is a key redox—active phenazine whose broad—spectrum bioactivity stems primarily from inducing intracellular oxidative stress (Abdelaziz et al., 2023). Pyocyanin has been reported to exert potent activity against *Candida* spp. (MIC = 38.5 µg/mL) (Oves et al., 2024) as well as significant mycelial inhibition against *Fusarium* spp. (Abdelaziz et al., 2023). In addition, 1—phenazinecarboxylic acid (PCA, m/z 224.05) was detected. This compound, alongside related phenazine derivatives (e.g., phenazine, 2—acetamidophenol, and aeruginaldehyde), markedly suppresses fungal spore germination and hyphal growth (Lu et al., 2024; Motta Escobar et al., 2022). The detection of biosynthetic precursors such as 1—hydroxy—2—nonenyl—1,4—dihydroquinolin—4—one and 6—phosphonoglucono—D—lactone further confirms active metabolic flux through the phenazine and pyocyanin pathways.

The metabolomic analysis also revealed 2,4—diacetylphloroglucinol (DAPG), a well—characterized polyketide antibiotic synthesized via the conserved *phlACBDEFGHI* gene cluster. DAPG exhibits strong antifungal efficacy against major phytopathogenic fungi, including *Fusarium oxysporum*, *Monilinia fructicola*, and *Botrytis cinerea* (Balthazar et al., 2022). Furthermore, the P38 extract contained lipid precursors associated with PVD maturation—notably myristic acid—and the secondary siderophore pyochelin.

Collectively, these metabolomic findings demonstrated that the antifungal activity of strain P38 is not restricted to pyoverdin—mediated iron competition alone. Instead, strain P38 secretes a multifaceted chemical arsenal comprising phenazines, polyketides, secondary siderophores, and quorum—sensing modulators. Cultivation in a low—phosphate, succinate—supplemented minimal medium (PM2) optimizes the expression of these co—regulated secondary metabolites, establishing strain P38 as a highly versatile and robust biocontrol candidate for crop protection.

Table 4. *Metabolites identified in* Pseudomonas *spp. and their potential antifungal activity*

m/z	**RT [min]**	**m/z BD *Pseudomonas* spp.**	**Compound name**	**Siderophore activity**	**Antifungal activity**
316.225	8.98	315.013	3-Deoxy-D-manno-octulosonate 8-phosphate		
		316.1	C11-PQS		X

325.066	7.829	324.035	Uridine 5'-monophosphate		
		324.024	5-O-(1-carboxyvinyl)-3-phosphosikimate		
		324.06	Pyocheline I	X	X
		324.06	Pyocheline II	X	X
		324.06	Pyocueline	X	X
258.146	7.877	258.110	Glycerophosphocholine		
		258.014	6-phosphonoglucono-D-lactone	X	
211.086	4.334	210.053	2-4-diacetil floroglucinol (DAPG)	X	
		211.087	Pyocyanin	X	
286.178	8.213	286.180	1-hydroxy-2-nonenyl-1.4-dihydroquinoline-4-one	X	
228.267	8.212	227.201	tetradecanoate (n-C14:0)		
		227.090	Deoxycytidine0		
		228.09	(1R.10aS)-1.4.10.10a-tetrahydrophenazine-1-carboxylic acid		X
		228.074	Deoxyuridine		
		228.208	Myristic acid		
225.065	7.786	224.058	1-Phenazine carboxylic acid	X	X

4. Conclusions

This study demonstrates that culture medium optimization—specifically utilizing succinic acid under low phosphate conditions (PM2 formulation)— significantly enhanced PVD yield and iron—chelating capacity

in native *Pseudomonas* sp. strains P07 and P38. Among the isolates, strain P38 showed a superior, iron—independent biocontrol profile, achieving potent mycelial growth inhibition against both *Colletotrichum* sp. (91.61%) and *Fusarium* sp. (91.39%). Both microdilution assays further revealed pathogen—specific antagonist mechanisms: while *Colletotrichum* sp. is markedly suppressed by chemical antibiosis via concentrated extracellular extracts (85.53% inhibition), effective biocontrol of *Fusarium* sp. relies predominantly on direct physiological competition with bacterial cells. Untargeted UHPLC—MS metabolomic profiling confirms that the high bioactivity of strain P38 is driven by a multifaceted secretome regulated by the C11—PQS quorum—sensing system, comprising secondary siderophores (pyochelin), redox—active phenazines (pyocyanin and 1—phenazinecarboxylic acid), polyketides (2,4—diacetylphloroglucinol), and pyoverdine maturation precursors (myristic acid). Overall, native *Pseudomonas* sp. strain P38 is a highly effective and versatile candidate for developing biocontrol tools for sustainable agricultural management.

5. Acknowledgments

The authors thank the Biociencias research group at Institución Universitaria Colegio Mayor de Antioquia and the Biotransformación research group at Universidad de Antioquia. We also thank the students and graduates of the Biotechnology and Industrial Microbiology programs at both institutions.

6. References

Abdelaziz, A. A., Kamer, A. M. A., Al-Monofy, K. B., & Al-Madboly, L. A. (2023). Pseudomonas aeruginosa's greenish-blue pigment pyocyanin: its production and biological activities. In *Microbial Cell Factories* (Vol. 22, Number 1). BioMed Central Ltd. https://doi.org/10.1186/s12934-023-02122-1

Abdelghani, Z., Hourani, N., Zaidan, Z., Dbaibo, G., Mrad, M., & Hage-Sleiman, R. (2021). Therapeutic applications and biological activities of bacterial bioactive extracts. In *Archives of Microbiology* (Vol. 203, Number 8, pp. 4755–4776). Springer Science and Business Media Deutschland GmbH. https://doi.org/10.1007/s00203-021-02505-1

Abdel-Razek, A. S., El-Naggar, M. E., Allam, A., Morsy, O. M., & Othman, S. I. (2020). Microbial natural products in drug discovery. In *Processes* (Vol. 8, Number 4). MDPI AG. https://doi.org/10.3390/PR8040470

Balthazar, C., St-Onge, R., Léger, G., Lamarre, S. G., Joly, D. L., & Filion, M. (2022). Pyoluteorin and 2,4-diacetylphloroglucinol are major contributors to Pseudomonas protegens Pf-5 biocontrol against Botrytis cinerea in cannabis. *Frontiers in Microbiology*, *13*. https://doi.org/10.3389/fmicb.2022.945498

Baukova, A., Bogun, A., Sushkova, S., Minkina, T., Mandzhieva, S., Alliluev, I., Jatav, H. S., Kalinitchenko, V., Rajput, V. D., & Delegan, Y. (2024). New Insights into Pseudomonas spp.-Produced Antibiotics: Genetic Regulation of Biosynthesis and Implementation in Biotechnology. In *Antibiotics* (Vol. 13, Number 7). Multidisciplinary Digital Publishing Institute (MDPI). https://doi.org/10.3390/antibiotics13070597

Bedoya Vélez, J. M., Castaño, G., & Ochoa Agudelo, S. (2019). Tolerancia al plomo de aislamientos nativos de Pseudomonas spp. de aguas residuales del Valle de Aburrá. *Revista Colombiana de Biotecnología*, *21*(1), 135–143. https://doi.org/10.15446/rev.colomb.biote.v21n1.65146

Bello, C., Tomás, S., & de Villegas, D. (2006). Purificación parcial del Pioverdin a partir de caldos de fermentación de Pseudomonas aeruginosa PSS. *ICIDCA*, (1). http://www.redalyc.org/articulo.oa?id=223121549006

Ch'ng, Y. R., Yong, C. S. Y., Othman, S. N., Zainudin, N. A. I. M., & Mustafa, M. (2022). Isolation and Molecular Identification of a Siderophore Producing Bacterium and its Antagonistic Effect Against Fusarium oxysporum f. sp. cubense Tropical Race 4. *Pertanika Journal of Tropical Agricultural Science*, *45*(1), 187–206. https://doi.org/10.47836/pjtas.45.1.11

Chung, P. C., Wu, H. Y., Wang, Y. W., Ariyawansa, H. A., Hu, H. P., Hung, T. H., Tzean, S. S., & Chung, C. L. (2020). Diversity and pathogenicity of Colletotrichum species causing strawberry anthracnose in Taiwan and description of a new species, Colletotrichum miaoliense sp. nov. *Scientific Reports*, *10*(1). https://doi.org/10.1038/s41598-020-70878-2

de Alvindia, D. G., & Mangoba, M. A. A. (2020). Bioactivities of Allium longicuspis Regel against anthracnose of mango caused by Colletotrichum gloeosporioides (Penz.). *Scientific Reports*, *10*(1). https://doi.org/10.1038/s41598-020-68399-z

Dell'Anno, F., Vitale, G. A., Buonocore, C., Vitale, L., Palma Esposito, F., Coppola, D., Della Sala, G., Tedesco, P., & de Pascale, D. (2022). Novel Insights on Pyoverdine: From Biosynthesis to Biotechnological Application. In *International Journal of Molecular Sciences* (Vol. 23, Number 19). MDPI. https://doi.org/10.3390/ijms231911507

Díaz-Pérez, S. P., Solis, C. S., López-Bucio, J. S., Valdez Alarcón, J. J., Villegas, J., Reyes-De la Cruz, H., & Campos-Garcia, J. (2022). Pathogenesis in Pseudomonas aeruginosa PAO1 Biofilm-Associated Is Dependent on the Pyoverdine and Pyocyanin Siderophores by Quorum Sensing Modulation. *Microbial Ecology*. https://doi.org/10.1007/s00248-022-02095-5

Dutta, S., Basak, R., & Chakraborty, S. (2022). ISOLATION AND DETERMINATION OF CHROMIUM (VI) AND NICKEL (II) RESISTANT SIDEROPHORE PRODUCING BACILLUS CEREUS(sp) AND ANALYSIS OF THE PROTEIN EXPRESSION USING BIOINFORMATICS TOOLS. *Journal of Microbiology, Biotechnology and Food Sciences*, *11*(6). https://doi.org/10.55251/jmbfs.3611

Ghssein, G., & Ezzeddine, Z. (2022). A Review of Pseudomonas aeruginosa Metallophores: Pyoverdine, Pyochelin and Pseudopaline. In *Biology* (Vol. 11, Number 12). MDPI. https://doi.org/10.3390/biology11121711

Gyawali, S., Bhattarai, G., Correll, J. C., Shi, A., & du Toit, L. J. (2025). Genome wide association study of Fusarium wilt resistance in Spinacia turkestanica. *Scientific Reports*, *15*(1). https://doi.org/10.1038/s41598-025-98932-x

Hussein, K. A., & Joo, J. H. (2017). Stimulation, purification, and chemical characterization of siderophores produced by the rhizospheric bacterial strain Pseudomonas putida. *Rhizosphere*, *4*, 16–21. https://doi.org/10.1016/j.rhisph.2017.05.006

Islam, M. A., Nain, Z., Alam, M. K., Banu, N. A., & Islam, M. R. (2018). In vitro study of biocontrol potential of rhizospheric pseudomonas aeruginosa against fusarium oxysporum f. Sp. cucumerinum. *Egyptian Journal of Biological Pest Control*, *28*(1), 1–11. https://doi.org/10.1186/s41938-018-0097-1

Jeong, G. J., Khan, F., Khan, S., Tabassum, N., Mehta, S., & Kim, Y. M. (2023). Pseudomonas aeruginosa virulence attenuation by inhibiting siderophore functions. In *Applied Microbiology and Biotechnology* (Vol. 107, Number 4, pp. 1019–1038). Springer Science and Business Media Deutschland GmbH. https://doi.org/10.1007/s00253-022-12347-6

Kejela, T., Thakkar, V. R., & Patel, R. R. (2017). A novel strain of Pseudomonas inhibits Colletotrichum gloeosporioides and Fusarium oxysporum infections and promotes germination of coffee. *Rhizosphere*, *4*, 9–15. https://doi.org/10.1016/j.rhisph.2017.05.002

Kim, J., Kim, J. C., & Sang, M. K. (2023). Identification of isomeric cyclo(leu-pro) produced by Pseudomonas sesami BC42 and its differential antifungal activities against Colletotrichum orbiculare. *Frontiers in Microbiology*, *14*. https://doi.org/10.3389/fmicb.2023.1230345

Kipgen, T. L., Bora, L. C., Goswami, G., Barooah, M., Borah, P. K., & Puzari, K. C. (2021). Isolation and characterization of fluorescent Pseudomonas with bio-control potential against Ralstonia solanacearum. *Indian Phytopathology*, *74*(4), 1055–1064. https://doi.org/10.1007/s42360-021-00400-9

Kumar, V., & Tiwari, S. K. (2017). Activity-guided separation and characterization of new halocin HA3 from fermented broth of Haloferax larsenii HA3. *Extremophiles*, *21*(3), 609–621. https://doi.org/10.1007/s00792-017-0930-6

Lu, J., Huang, Y., Liu, R., Liang, Y., Zhang, H., Shen, N., Yang, D., & Jiang, M. (2024). Antimicrobial mechanisms and antifungal activity of compounds generated by banana rhizosphere Pseudomonas aeruginosa Gxun-2 against fusarium oxysporum f. sp. cubense. *Frontiers in Microbiology*, *15*. https://doi.org/10.3389/fmicb.2024.1456847

Ma, Z., Liu, F., Tsui, C. K. M., & Cai, L. (2025). Phylogenomics and adaptive evolution of the Colletotrichum gloeosporioides species complex. *Communications Biology*, *8*(1). https://doi.org/10.1038/s42003-025-08024-9

Motta Escobar, S., Salazar Cabezas, L. D., & Sánchez Leal, L. C. (2022). Perspectiva del uso de Pseudomonas spp. como biocontrol de fitopatógenos en cultivos de hortalizas en Colombia: una revisión sistemática. *Revista Mutis*, *12*(2). https://doi.org/10.21789/22561498.1862

Murakami, C., Tanaka, A. R., Sato, Y., Kimura, Y., & Morimoto, K. (2021). Easy detection of siderophore production in diluted growth media using an improved CAS reagent. *Journal of Microbiological Methods*, *189*. https://doi.org/10.1016/j.mimet.2021.106310

Nair, A., Juwarkar, A. A., & Singh, S. K. (2007). Production and characterization of siderophores and its application in arsenic removal from contaminated soil. *Water, Air, and Soil Pollution*, *180*(1–4), 199–212. https://doi.org/10.1007/s11270-006-9263-2

Oves, M., Khan, M. S., Al-Shaeri, M., & Khan, M. S. (2024). Antifungal potential of multi-drug-resistant Pseudomonas aeruginosa: harnessing pyocyanin for candida growth inhibition. *Frontiers in Cellular and Infection Microbiology*, *14*. https://doi.org/10.3389/fcimb.2024.1375872

Purohit, A., Ghosh, S., Ganguly, S., Negi, M. S., Tripathi, S. B., Chaudhuri, R. K., & Chakraborti, D. (2021). Comparative transcriptomic profiling of susceptible and resistant cultivars of pigeonpea demonstrates early molecular responses during Fusarium udum infection. *Scientific Reports*, *11*(1). https://doi.org/10.1038/s41598-021-01587-7

Rani, L., Srivastav, A. L., & Kaushal, J. (2021). Bioremediation: An effective approach of mercury removal from the aqueous solutions. *Chemosphere*, *280*(April), 130654. https://doi.org/10.1016/j.chemosphere.2021.130654

Rehm, K., Vollenweider, V., Kümmerli, R., & Bigler, L. (2022). Rapid identification of pyoverdines of fluorescent Pseudomonas spp. by UHPLC-IM-MS. *BioMetals*. https://doi.org/10.1007/s10534-022-00454-w

Sarvepalli, M., Velidandi, A., & Korrapati, N. (2023). Optimization of Siderophore Production in Three Marine Bacterial Isolates along with Their Heavy-Metal Chelation and Seed Germination Potential Determination. *Microorganisms*, *11*(12). https://doi.org/10.3390/microorganisms11122873

Sasirekha, B., & Srividya, S. (2016). Siderophore production by Pseudomonas aeruginosa FP6 , a biocontrol strain for Rhizoctonia solani and Colletotrichum gloeosporioides causing diseases in chilli. *Agriculture and Natural Resources*, *50*(4), 250–256. https://doi.org/10.1016/j.anres.2016.02.003

Schwyn, B., & Neilands, J. B. (1987). Universal chemical assay for the detection and determination of siderophores. *Analytical Biochemistry*, *160*(1). https://doi.org/https://doi.org/10.1016/0003-2697(87)90612-9

Soares, E. V. (2022). Perspective on the biotechnological production of bacterial siderophores and their use. In *Applied Microbiology and Biotechnology* (Vol. 106, Number 11, pp. 3985–4004). Springer Science and Business Media Deutschland GmbH. https://doi.org/10.1007/s00253-022-11995-y

Song, Z., Liu, Y., Gao, J., Hu, J., He, H., Dai, S., Wang, L., Dai, H., Zhang, L., & Song, F. (2021). Antitubercular metabolites from the marine-derived fungus strain Aspergillus fumigatus MF029. *Natural Product Research*, *35*(16), 2647–2654. https://doi.org/10.1080/14786419.2019.1660331

Swayambhu, G., Bruno, M., Gulick, A. M., & Pfeifer, B. A. (2021). Siderophore natural products as pharmaceutical agents. In *Current Opinion in Biotechnology* (Vol. 69, pp. 242–251). Elsevier Ltd. https://doi.org/10.1016/j.copbio.2021.01.021

Tapia P., C. V. (2009). Actualización en pruebas de susceptibilidad antifúngica. *Revista Chilena de Infectología*, *26*(2). https://doi.org/http://dx.doi.org/10.4067/S0716-10182009000200005

Vindeirinho, J. M., Soares, H. M. V. M., & Soares, E. V. (2021). Modulation of Siderophore Production by Pseudomonas fluorescens Through the Manipulation of the Culture Medium Composition. *Applied Biochemistry and Biotechnology*, *193*(3), 607–618. https://doi.org/10.1007/s12010-020-03349-z